LAND-USE CLASSIFICATION OF AERIAL IMAGES USING ARTIFICIAL

NEURAL NETWORKS

by

DEV ASHISH

(Under the direction of RONALD W. McCLENDON)

ABSTRACT

This thesis describes the study of Artificial Neural Network (ANN) based techniques for the classification of aerial images for various types of land-use. In this study both gray-scale and multispectral aerial images were used in land-use classification. Three approaches were used for the preparation of the data as inputs to the ANN, including histograms of the pixel intensities, textural parameters extracted from the image, and matrices of pixels for spatial information. The approach using textural parameters was found to be the best for both gray-scale and multispectral image classification. A probabilistic neural network was employed. A high level of accuracy was achieved with both gray-scale (92%) and multispectral images (89%).

INDEX WORDS: Aerial remote sensing, artificial neural networks, image classification, image processing.

LAND-USE CLASSIFICATION OF AERIAL IMAGES USING ARTIFICIAL

NEURAL NETWORKS

by

DEV ASHISH

B.Sc., Punjab University, India, 1995

M.Sc., Punjab University, India, 1997

M.Tech., Guru Jambheshwar University, India, 1999

A Thesis Submitted to the Graduate Faculty of The University of Georgia in Partial

Fulfillment of the Requirement for the Degree

MASTER OF SCIENCE

ATHENS, GEORGIA

2002

LAND-USE CLASSIFICATION OF AERIAL IMAGES USING ARTIFICIAL

NEURAL NETWORKS

by

DEV ASHISH

Approved:

Major Professor: Ronald W. McClendon

Committee: Gerrit Hoogenboom
                     Walter D. Potter

Electronic Version Approved:

Gordhan L. Patel
Dean of the Graduate School
The University of Georgia
August 2002

DEDICATION

To all my *angels*...

ACKNOWLEDGEMENTS

TABLE OF CONTENTS

CHAPTER 1

INTRODUCTION

The goal of this thesis was to develop a land-use classification scheme for remotely sensed aerial images to aid in agricultural production decision support and policymaking. This research explored the use of both gray-scale and multispectral aerial images. The specific objectives in each of these efforts included the comparison of different approaches for preparing data for classification using artificial neural networks. The three approaches used for the preparation of the inputs to the artificial neural network (ANN) included histograms of the pixel intensities, textural parameters extracted from the image, and matrices of pixels for spatial information.

The ANN based technique used for the land-use classification of gray-scale aerial images is discussed in Chapter 2. Chapter 3 discusses land-use classification using multispectral images. Chapter 4 summarizes the results of the tests and discusses the overall performance of the ANNs.

1.1 Remote sensing and image classification

In order to gather and interpret geo-spatial data, remote sensing technology that employs different radiation spectra is used. This technology is applicable in developing information about features, objects, and classes for the earth's land surface, oceans, and

the atmosphere. With the recent advances in remote sensing high resolution data are available at short time intervals. For instance, the Landsat 7 satellite operated by United States Geological Survey (USGS) can provide remote sensing data in a 16-day repeat cycle from a panchromatic band with 15-meter spatial resolution (Short, 1999). The SPOT 5 satellite has up to a 2.5-meter ground resolution in panchromatic mode with a 26-day repeat cycle (Short 1999). However, aerial images can achieve even higher resolutions, depending on the type of sensor that is being used. The cost of high-resolution images has become comparatively low and images are more readily available due to advances in sensing techniques and commercialization of many of these technologies.

Another major advancement in remote sensing has been in the field of imaging spectroscopy. Remote sensors that cover two thermal intervals corresponding to two atmospheric windows allow sensing of thermal emissions from land, water, ice and the atmosphere. The sensors have been flown on airplanes for several decades. Many of the meteorological satellites include at least one thermal channel with other sensors. A thermal band has also been included on the Landsat Thematic Mapper. Radar systems are another class of satellite remote sensors that are currently operational in space. A radar normally provides a very different view of the same landscape compared to a visible image because of its ability (for certain wavelengths) to penetrate clouds. Seasat, the Spaceborne Imaging Radar (SIR) series, and Radarsat are among the instruments used so far. The Multispectral Scanner (MSS) has been the most important sensor that was part of the first five Landsats. The Landsat MSS gathers radiation over spectral band widths that integrate radiation over relatively broad intervals (0.1 and 0.3 μm). Thus, instead of the

spectral signatures that continuously measure spectral response in very narrow intervals, the MSS data when plotted produce histogram-like bars that are rough approximations of the signature curves. Hyperspectral imaging is a powerful and versatile means for continuous sampling of broad intervals of the spectrum. Hyperspectral imaging allows a sensor on a moving platform to gather reflected radiation from a ground target such that a special detector system can record up to 217 spectral channels (each approximately 10 nanometers in width) simultaneously over the range from 0.38 to 2.5 mm. With such detail, the ability to detect and identify individual materials or classes greatly improves.

Image classification is a key component of remote sensing (Baraldi and Parmiggiani, 1990; Biscoff et al., 1992; Carmel and Kadmon 1998). Image classification is the process of creating thematic maps from satellite imagery. A thematic map is an informational representation of an image, which shows the spatial distribution of a particular theme. An example of themes could be vegetation types consisting of trees, crops, grasslands, etc. Finer sub-themes can also be defined inside a theme to make the process of classification more refined, such as classifying trees as deciduous or evergreen. Image classification relies on the spectral distinctness of classes or spectro-temporal variability. It also depends on the context of classification. For example, two features with nearly identical spectral signatures for vegetation could be assigned to the classes 'forest' and 'crops' depending on whether the area in the images has irregular or straight boundaries. Various studies reported a very high accuracy in image classification (Ritter and Hepner, 1990; Chen, 1995; Du, 1996; Carmel and Kandmon, 1998; Tsai, 2002). However, it is vital to extend techniques to further improve remote sensing image classification accuracy for

deriving dependable land cover information for vegetation, land-use and other applications.

Gray-scale images are single spectrum images, whereas multispectral images use more than one spectrum. In gray-scale pictures, the information that can be retrieved from the image is the intensity of the pixels and the relative position of the pixels. Most land-use classes have a characteristic value for intensity, which is used in generating spectral classes from image classification. The spatial composition of these spectral classes within a certain spatial range can be useful information for image classification (Fung and Chan, 1994). Images can also be classified based on texture information from the image. Several parameters related to the texture recognition of an image were proposed by Haralick (1973). These include angular second moment, contrast, correlation, inverse difference moment, and entropy. Angular second moment is a measure of the homogeneity of the image. Contrast is a measure of the amount of local variation present in an image. Correlation is a measure of gray-tone linear-dependencies in the image. Inverse difference moment is a measure of the amount of local similarity. Entropy is a measure of the average uncertainty of gray tone co-occurrence in the image. Contrast, entropy, angular second moment and inverse difference moment have been widely used for image classification and image analysis. Jensen (1979) applied these Haralick's measures to Landsat images for land cover classification and achieved up to 80% accuracy. Marceau et al. (1990) used the same Haralick's textural parameters for land-cover classification of nine land-cover types in SPOT imagery and achieved up to 100% accuracy for some land-cover types. Kondo et al. (2000) used the Haralick's parameters for evaluating sugar and acid content of Iyokan orange fruit based on a

machine vision system. Singh and Singh (2001) compared several texture methods for image analysis. The performance evaluation was based on the ability of a classifier to recognize unseen samples of the four classes on the basis of training data. The best overall result using nearest neighbour methods was obtained with Haralick's parameters based on co-occurrence matrices.

1.2 Artificial neural network and image classification

Artificial neural networks (ANNs) are computational mathematical models that emulate some of the observed properties of biological neural systems and draw on the analogies of adaptive biological learning. An ANN is composed of a number of interconnected processing elements that are similar to neurons. These processing elements are joined by weighted connections that are analogous to synapses in the human brain. Supervised learning in an ANN typically occurs by example through training or exposure to a known set of input and corresponding output data. The training algorithm adjusts the connection weights through an iterative procedure in which the error is minimized. The superiority of ANNs to some of the classical statistical methods in various problems, including classification problems, has been shown in the previous studies (Bischof et al., 1990; Paola and Schowengerdt, 1995; Blackard and Dean, 1999; Giraudel, 2001). ANNs are commonly used for segmentation and classification purposes and are recommended for problems where data diversity is large (Lee et al., 1990; Warner and Shank, 1997; Moshou, 2001).

The viability of land-use classification of remotely sensed image areas with ANNs was established by Benediktsson et al. (1990). Subsequent studies that examined the

neural network classifier method in more detail also compared it to standard statistical classification techniques (Paola and Schowengerdt, 1995; Luo et al., 1997; Zhang and Foody, 2001). These studies presented several classification approaches that are based on ANNs, such as the pixel-by-pixel or per-pixel method (Salu and Tilton, 1993). The pixel-by-pixel method deals with classification of pixels. The classification aims at attributing each pixel to its correct land cover category. The dimensions of pixels are usually related to the field of view of the sensor that obtained the image, and the sampling rate of the analogue-to-digital converter used to translate the signal received at the detector. It is hypothesized that the statistical characteristics of a group of pixels can be used to define a decision rule for discrimination between the cover type of that pixel and all others. However, this approach faces several difficulties due to the interaction between light and the components of atmosphere and due to the geometry of the imaging system (Mather, 1990). The per-pixel method is also not appropriate for classification high resolution images because the spatial variability of surface features increases with the increase in spatial resolution (Marceau et al., 1990). Higher variability diminishes classification accuracies (Irons et al., 1985).

Previously, most of the research for land-use classification has focused on the analysis of multispectral images (Bischof et al., 1992; Civco and Waug, 1994; Schultz et al., 2000). Only a few applications are based on gray-scale images (Metzler et al., 2000) and no comparisons have been made with multispectral data analysis. Accurate classification of gray-scale images into various land-uses is challenging because of the limited spectral information that is provided in these images, as discussed previously. There have been several new approaches, such as the contextual classification scheme

and methods based on fuzzy sets or their combinations, which have had better success than usual methods. Contextual classifiers increase the dimensionality of data with additional bands in which contextual information is present in some way or assume the existence of local properties defined on a neighborhood where the spatial dependence is relevant. The fuzzy approach, proposed by Wang (1990), allow for multiple and partial classification of mixed pixels. This approach gives more information on the relative strengths of class membership at the pixel level. Gong and Howarth (1992) found that the contextual classification for land-use classification of SPOT HRV data better than the conventional maximum likelihood classification method. Cortijo and De la Blanca (1998) achieved 91% accuracy with contextual classification. Papin (2002) demonstrated the accuracy and efficiency of the contextual approach. Gopal and Woodcock (1994) successfully used fuzzy sets for accuracy assessment of thematic maps. Zhang and Foody (2001) used fully-fuzzy supervised classification to determine land cover based on images obtained from Landsat Thematic Mapper and obtained better results than partially fuzzy classification.

CHAPTER 2

LAND-USE CLASSIFICATION OF GRAY-SCALE AERIAL IMAGES USING

ARTIFICIAL NEURAL NETWORKS[1]

Abstract—With the advancement in remote sensing methods that can provide high resolution data at shorter intervals, it has become important to develop classification methodologies to exploit these technologies. The objective of this study was to develop an Artificial Neural Network (ANN) based technique for the classification of gray-scale aerial images into various types of land-use, especially for rural areas where agriculture is important. We defined specific land-use classes including city, water, forest and various types of agricultural field areas. Gray-scale aerial images with a 6.5-meter resolution for nine counties were obtained. Three approaches were used for the preparation of the inputs to the ANN, including histograms of the pixel intensities, textural parameters extracted from the image, and matrices of pixels for spatial information. A probabilistic neural network was used in this study. Twelve hundred images were used for model development and 300 for model evaluation. The best ANN was based on textural parameters and achieved an overall accuracy of 92% for the evaluation data set. Overall accuracy for the spatial approach was 66% for the evaluation data set. Combinations of all three approaches were also evaluated without an improvement in accuracy.

Index Terms— Aerial remote sensing, artificial neural networks, image classification, image processing.

2.1. Introduction

Remote sensing is a technology that uses different radiation spectra to acquire and interpret geo-spatial data. This information can then be used to develop information about features, objects, and classes for the earth's land surface, oceans, and atmosphere. Remote sensing can be classified into either aerial or satellite based techniques, depending on the

9

platform used for sensors. Image classification is a key component of remote sensing and relies on the spectral distinctness of classes and/or spectro-temporal variability and the context of classification [1], [2], [24] [27]. None of the previous studies have achieved complete accuracy in classification. The development of techniques to improve remote sensing image classification accuracy is essential for deriving reliable land cover information for vegetation, land-use and other applications.

High resolution images are now readily available at a relatively low cost. References [8] and [25] found high-resolution images more suitable for land-use classification compared to low-resolution images, as they contain more information per pixel. Images can broadly be grouped into two categories depending on the number of spectra. Gray-scale images are single spectrum images, whereas multispectral images use more than one spectrum. In gray-scale pictures, the information that can be retrieved from the image is the intensity of the pixels and the relative position of the pixels. Most land-use classes have a characteristic value for intensity, but it is difficult to determine the various classes based solely on intensity values because of the absence of spatial information.

Texture is another important characteristic that is used in classifying gray-scale images. Reference [9] proposed several parameters to identify the texture of an image. These textural parameters include angular second moment, contrast, correlation, inverse difference moment, and variance. Angular second moment is a measure of the homogeneity of the image. Contrast is a measure of the amount of local variation present in an image. Inverse difference moment is a measure of the amount of local similarity. Correlation is a measure of gray-scale linear-dependencies in the image. Contrast, angular second moment and inverse difference moment have been widely used for image classification [12], [16].

Artificial neural networks (ANNs) are computational mathematical models that emulate some of the observed properties of biological neural systems and draw on the analogies of adaptive biological learning. An ANN is composed of a number of interconnected processing elements that are similar to neurons. These processing elements are joined by weighted connections that are analogous to synapses. Supervised learning in an ANN typically occurs by example through training or exposure to a known set of input and corresponding output data. The training algorithm adjusts the connection weights through an iterative procedure in which the error is minimized. The superiority of ANNs to some of the classical statistical methods in various problems has been shown in the literature [3], [19]. ANNs are commonly used for segmentation and classification purposes and are recommended for problems where data diversity is large [4], [11], [17], [21], [26].

Reference [2] established the feasibility of land-use classification of remotely sensed image areas with ANNs. Subsequent studies examined the neural network classifier method in more detail and compared it to standard statistical classification techniques [13], [19], [30]. Previously, most of the research for land-use classification has focused on the analysis of multispectral images [3], [5], [20]. Only a few applications are based on gray-scale images [16] and no comparisons have been made with multispectral data analysis. Accurate classification of gray-scale images into various land-uses is challenging because of the limited spectral information that is provided in these images, as discussed previously.

Several classification approaches that are based on ANNs have been presented, such as the pixel-by-pixel or per-pixel method [20]. In the pixel-by-pixel method, each pixel of the remotely sensed image is classified. The dimensions of pixels are usually related to

the field of view of the instrument that obtained the image, and the sampling rate of the analogue-to-digital converter used to translate the signal received at the detector. It is assumed that the statistical characteristics of a group of pixels can be used to define a decision rule for discrimination between the cover type of that pixel and all others. However, this approach faces several difficulties due to the effects of interactions between light and the components of atmosphere and due to the effect of the geometry of the imaging system [15]. New approaches such as the contextual classification scheme [6] and methods based on fuzzy sets [7] have been used with better success than conventional methods.

The overall goal of our research was to develop a land-use classification scheme for remotely sensed images to aid in agricultural production decision support and policymaking. The three approaches considered include the use of histograms of the pixel intensities, textural parameters extracted from the image and spatial matrices of pixels for spatial information. Gray-scale images were used because they are available for the entire state of Georgia. Multispectral images are currently available only for limited regions, usually metropolitan areas, and our focus was on agricultural land-use.

2.2. Methods and materials

Gray-scale aerial images were obtained from the Georgia GIS Data Clearinghouse website for the entire state of Georgia (http://www.ganet.org/gis/chouse). Images from Baker, Bibb, Clarke, Colquitt, Fulton, Houston, Macon, Mitchell, and Seminole counties were used in this study. These high-resolution gray-scale aerial images are georeferenced and geocorrected. Most of this imagery was taken in 1993 and it is generally known as Digital Orthophotography Quarter-Quadrangles (DOQQs). The online versions of the

DOQQs have been resampled to 6.5-meter resolution in a JPEG image format. The Georgia GIS Data Clearinghouse also has multispectral images of the same resolution only for several counties in the greater Atlanta Metropolitan area.

For this study gray-scale aerial pictures were downloaded in JPEG format from the Georgia GIS Data Clearinghouse. Small subareas of known classes, called "images", were manually selected using the software Paintshop Pro (version 6.00). Images had different sizes due to the selection process (fig. 1.1). These images were visually separated into six different classes, including city, forest, water, dark field, medium dark field and light field. For the manual selection of images for various field classes, the mean pixel intensity of the image was used for a limited number of images in the dark, medium dark and light field classes. Each one of the six classes was represented by 250 images for a total of 1500 images. Of the total, 200 images from each class were used for model development, which included 150 images for training and 50 images for testing. The remaining 50 images from each class were separated for later use in the evaluation data set for final evaluation of the ANN model. The training set consisted of patterns used to adjust the weights to minimize the error and the test set was used periodically in feed forward mode only to determine when to stop training to avoid overfitting. The evaluation set was used to evaluate the accuracy of the model once training was completed.

In the first approach, histograms of pixel intensities (fig. 2.1) were created from the pixel values of the image. They were then normalized based on the number of pixels from the entire image in order to allow for a comparison of images of different sizes. For the second approach, the spatial information of an image was extracted from the central part of the image. This spatial information corresponds to the intensity of the pixels in the

specific spatial order to preserve their spatial location in the grid. The central portion of the image used for extracting preprocessed information is termed a "window" herein. In the third approach, textural parameters were calculated from the pixel data of the image (or the central portion of the image) according to different methods proposed by [9]. The Haralick's textural parameters used in this study were angular second moment (ASM) and inverse difference moment (IDM). These are the most frequently used parameters [10], [12], [22] and found to have the best performance among textural parameters [18], [22]. In addition, the mean and standard deviation of pixel intensities were also calculated.

$$ASM = \sum_i \sum_j \{p(i,j)\}^2 \qquad (1)$$

$$IDM = \sum_i \sum_j \frac{1}{1+(i-j)^2} p(i,j) \qquad (2)$$

where *p(i,j)* is a value in co-occurrence matrix which represents the number of times pixel *a* has a value *i* and pixel *b* has value *j* when pixel *a* is a neighbor of pixel *b*, *a* and *b* varying over the entire image.

After preprocessing, the data were presented to an ANN for training using one of the approaches previously described. The software Neuroshell 2 (release 3), developed by Ward System Group Inc., was used in this study. In the preliminary tests the Probabilistic Neural Network (PNN) was found to have a higher accuracy than the standard back propagation algorithm and was therefore applied in all subsequent model development. The number of hidden layer neurons was equal to the number of patterns in the training set. The output layer in a PNN has the same number of neurons as the number of classes. The city class consisted of images of buildings and their neighboring areas. The forest class consisted of images taken from tree-covered regions. The water class images were

taken from lakes, ponds and rivers. The dark field class consisted of images of lush vegetation areas, whereas the medium dark field class consisted of images of relatively less dense vegetation areas. The light field class consisted of images of uncropped or fallow field areas.

The best ANN was selected based on the highest overall accuracy for the evaluation data set, which is a function of the performance of the ANN for all the individual classification classes. The overall accuracy was calculated from the error matrix of the classification results [23]. Overall accuracy is the ratio of the sum of correctly classified patterns of all the classes over the total number of patterns presented to the ANN. The error matrix can also provide information about the producer's and user's accuracy. Producer's accuracy is the ratio of the number of correctly classified patterns of a class over the total number of patterns of that class presented to the network. User's accuracy is the ratio of number of correctly classified patterns into a class over the total number of patterns classified as being in that class.

Each of the three approaches was considered individually with the same data sets. In the textural approach, there were four different parameters used as input for textural information. A separate study was performed to determine if any one or more of the inputs could be eliminated and still obtain the same level of accuracy. After testing all three approaches individually, a study was conducted considering various combinations of approaches in order to determine if this could further improve the accuracy.

2.3. Results and discussion

Histogram:

A comparative study was conducted for histograms of 64, 128 and 256 cells as shown in Table 2.1. The overall accuracy of the network for the 64-cell histogram was 89% for the evaluation data set. The 128-cell network had an overall accuracy of 90% which was slightly higher than the other two cases considered. Overall, the histogram based neural network performed well, except for the dark field and water classes. From Table 2.2, we can see the low producer's accuracy for dark field and water classes for the ANN with histogram approach. Out of 50 dark field images, nine were classified as forest and five as water. Six water images were classified as dark field. This misclassification between two classes with pixel intensity in same range could be due to lack of spatial or textural information. Relatively lower user's accuracy for forest (81%), dark field (83%) and water (85%) classes were observed.

Spatial:

The effect of various window sizes of the spatial matrix presented to the network was examined. The size of the window was limited to a maximum of 15x15 pixels, because the smallest images extracted were of the order of 15x15 pixels. The window sizes used were 1x1, 3x3, 5x5, 10x10, and 15x15 pixels. The ANN based on the 3x3 pixel window resulted in the highest overall accuracy of 66% (Table 2.3). These tests also showed that the overall performance of the network was reduced for window sizes larger than 3x3. However, the results of the individual classes varied considerably. The highest accuracy for forest (58%) and medium dark field (98%) was for a 5x5 pixel window and the highest for light field (100%) was for both 10x10 and 15x15 pixel windows. The city,

16

forest and dark field classes showed the worst performance. Fourteen city class images were classified as light field class, possibly due to the similar intensities and spatial distribution of the pixels for both (Table 2.4). Similarly, the forest and dark field classes also have similar intensities and spatial distribution, whereas different texture, which likely resulted in confusion.

Textural parameters:

A comparative study was conducted between various window sizes for the textural parameter approach. The two Haralick's textural parameters (angular second moment and inverse difference moment), mean and standard deviation of pixel intensity were used. The window sizes that were analyzed included 3x3, 5x5, 10x10, and 15x15 pixels and the full image. The entire image had the best performance with an overall accuracy of 92% for the evaluation data set (Table 2.5). The dark field (80%) and water class (84%) still had a relatively low producer's accuracy as compared to other classes (Table 2.6). Six dark field images were misclassified as forest and five water images were misclassified as the dark field class.

Since the textural approach delivered the highest overall accuracy, another study was conducted in which different combinations of textural parameters, such as angular second moment and inverse difference moment, and mean and standard deviation of pixel intensity, from the entire image were compared. The network based on a combination of angular second moment and inverse difference moment yielded an overall accuracy of only 58% (Table 2.7). The performance of the network using a combination of angular second moment, inverse difference moment and mean of pixel intensities performed the best among these networks (89%). The network based on a combination of mean and

standard deviation of pixel intensities had an accuracy of 82%, whereas the network based on a combination of angular second moment, inverse difference moment and standard deviation of pixel intensities had an accuracy of 72%. The better performance using a combination of mean and standard deviation of pixel intensities can also be attributed to the fact that mean pixel intensity was used as one of the criteria for manually classifying some of the images. The network based on all four textural parameters from the entire image still provided the highest overall accuracy.

Combinations of Histogram, Textural and Spatial information:

After analyzing the three approaches individually, they were evaluated in combination. Previously it was shown that the best performance was obtained based on textural parameters. In the first combination, the textural approach and histogram approach were evaluated. The textural information was obtained from a full image and the histogram was based on 128 cells, because these showed the best performance individually in earlier tests. The ANN based on a combination of textural parameters and histogram approaches had an overall accuracy of 88% for the evaluation set (Table 2.8). This accuracy was less than the overall accuracy of the ANN using textural parameters only (92%). The performance of the combined ANN for the dark field class (54%) was lower than for the ANN based on textural parameters only (80%).

In the second analysis, the performance of textural information in combination with spatial information was considered. The ANN was based on textural parameter for the entire image in combination with a 3x3 pixel window for spatial information. This ANN had an overall accuracy of 88% for the evaluation set, which again was less than the overall accuracy of the ANN that was based on textural parameter (92%) only.

In the third analysis, the performance of spatial information was tested in combination with histogram information. The ANN was based on a network using a combination of 128 cell histogram values and 3x3 window for spatial information. This ANN had an overall accuracy of 89% for the evaluation set. This again was less than the overall accuracy of the ANN that was based on textural parameters only from entire image (92%).

In the final analysis, an ANN based on a combination of textural, spatial and histogram information was evaluated. The textural information was obtained from the full image, the spatial information was obtained from the central 3x3 window and the 128-cells histogram was used. This ANN had an overall accuracy of 89% for the evaluation set, which was again less than the overall accuracy of the ANN that was based on textural parameters only. The producer's accuracy for the dark field class was much less (66%) than the producer's accuracy in the case of textural parameters alone, but the performance for the water class improved (92%).

The ANN based solely on textural parameters had the highest overall accuracy of 92% for the evaluation data set. It also had the smallest standard deviation (8%) for the producer's accuracy. An overall accuracy of 92% for the classification of gray-scale images using ANNs for land-use is similar to previous observations by [19] and [29]. The better performance of textural approach for gray-scale images compared to other approaches also strengthens the results of previous studies based on textural approaches on gray-scale and multispectral images [14], [22], [28].

2.4. Summary and conclusions

Good results were obtained for an ANN-based classification methodology of aerial gray-scale images for six land-use classes. The highest overall accuracy of 92% was achieved based on the textural parameters for classification, compared to approaches based on histogram and spatial information. This study further established the importance of the use of textural parameters for the classification of remotely sensed images. Low producer's and user's accuracy of dark field and its misclassification into the forest class can be of concern for some users, but further analysis of higher resolution images could further improve the results. The misclassification of water into dark field class can possibly be solved with the analysis of multispectral images. Multispectral image analysis may also provide better results for other classes.

References

[1] T. Akiyama, Y. Inoue, M. Shibayama, Y. Awaya, and N. Tanaka, "Monitoring and predicting crop growth and analysing agricultural ecosystems by remote sensing," *Agricultural and Food Science in Finland*, vol. 5, pp. 367-376, 1996.

[2] J. A. Benediktsson, P. H. Swain, and O. K. Ersoy, "Neural network approaches versus statistical methods in classification of multisource remote sensing data," *IEEE Transactions on Geoscience and Remote Sensing*, vol. 28, no. 4, pp. 540-551, July, 1990.

[3] H. Bischof, W. Schneider, and A. J. Pinz, "Multispectral classification of Landsat-images using neural networks," *IEEE Transactions on Geoscience and Remote Sensing*, vol. 30, no. 3, pp. 482-490, May, 1992.

[4] T. F. Burks, S. A. Shearer, R. S. Gates, and K. D. Donohue, "Backpropagation neural network design and evaluation for classifying weed species using color image texture features," Presented at the 1999 ASAE/CSAE-SCGR Annual International Meeting, ASAE, 2950 Niles Road, St. Joseph, MI, USA, Paper 993047.

[5] D. L. Civco and Y. Waug, "Classification of multispectral, multitemporal, multisource spatial data using artificial neural networks," in *Proc. 1994 Annual ASPRS/ACSM Convention, Reno, NV, USA*, pp. 123-133.

[6] F. J. Cortijo and N. P. De la Blanca, "Improving classical contextual classifications," *International Journal Of Remote Sensing*, vol. 19, no. 8, pp.1591-1613, 1998.

[7] S. Gopal, C. E. Woodcock, and A. H. Strahler, "Fuzzy neural network classification of global land cover from a 1 degree AVHRR data set," *Remote Sens. Environ.*, vol. 67, pp. 230-243, 1999.

[8] S. Gopalapillai and L. Tian, "In-field variability detection and spatial yield modeling for corn using digital aerial imaging," *Transactions of the ASAE*, vol. 42, no. 6, pp. 1911-1920, 1999.

[9] R. M. Haralick, K. Shanmugam, and I. Dinstein, "Textural features for image classification," *IEEE Transactions on System, Man, and Cybernetics*, vol. SMC-3, no. 6, pp. 610-621, November, 1973.

[10]   H. He and C. Collet, "Combining spectral and textural features for multispectral image classification with artificial neural networks," *International Archives of Photogrammetry and Remote Sensing*, Valladolid, Spain, vol. 32 part 7-4-3 W6, 1999.

[11]   S. Kamata and E. Kawaguchi, "A neural classifier for multi-temporal Landsat images using spatial and spectral information," in *Proceedings of 1993 International Joint Conference on Neural Networks*, Nagoya, Japan , pp. 2199-2202.

[12]   N. Kondo, U. Ahmad, M. Monta, and H. Murase, "Machine vision based quality evaluation of Iyokan orange fruit using neural networks," *Computer and Electronics in Agriculture*, vol. 29, pp. 135-147, 2000.

[13]   X. Luo, D. S. Jayas, and S. J. Symons, "Comparison of statistical and neural network methods for classifying cereal grains using machine vision," *Transactions of the ASAE*, vol. 42, no. 2, pp. 413-419, 1999.

[14]   D. J. Marceau, P. J. Howarth, J. M. Dubois, and D. J. Gratton, "Evaluation of the gray-level co-occurrence matrix method for land cover classification using SPOT imagery," *IEEE Transactions on Geoscience and Remote Sensing*, vol. 28, no. 4, pp. 513-519, July, 1990.

[15]   P. M. Mather, "Theoretical problems in image classification," in *Application of Remote Sensing in Agriculture*, J. A. Clark and M. D. Sevens, Ed. London: Butterworths, 1990, p 127-135.

[16]   V. Metzler, C. Palm, T. Lehmann, and T. Aach, "Texture classification of graylevel images by multi cross-coocurrence matrices," in *Proc. 15th International Conference on Pattern Recognition*, Barcelona, Spain , 2000, pp. 549-552.

[17]   D. Moshou, E. Vrindts, B. De Ketelaere, J. De Baerdemaeker, and H. Ramon, "A neural network based plant classifier," *Computer and Electronics in Agriculture*, vol. 31, no.1, pp. 5-16, 2001.

[18]   P. P. Ohanian and R. C. Dubes, "Performance evaluation for four classes of textural features," *Pattern Recognition*, vol. 25, no. 8, pp. 819-833, 1992.

[19]   J. D. Paola and R. A. Schowengerdt, "A detailed comparison of neural network and maximum likelihood classifiers for urban land use classification," *IEEE Transactions on Geoscience and Remote Sensing*, vol. 33, no. 4, pp. 981-996, July, 1995.

[20]   Y. Salu and J. Tilton, "Classification of multispectral image data by the binary diamond neural network and by nonparametric, pixel-by-pixel methods," *IEEE Transactions on Geoscience and Remote Sensing*, vol. 31, no. 3, pp. 606-617, May, 1993.

[21]   A. Schultz, R. Wieland, and G. Lutze, "Neural network in agroecological modeling – stylish application or helpful tool?," *Computers and Electronics in Agriculture*, vol. 29, pp. 73-97, 2000.

[22]   M. Singh and S. Singh, "Evaluation of texture methods for image analysis," in *Proc. 7th Australian and New Zealand Intelligent Information Systems Conference*, Perth, 2001, pp. 117-121.

[23]   M. Story and R. G. Congalton, "Accuracy assessment: a user's perspective," *Photogrammetric Engineering and Remote Sensing*, vol. 52, no. 3, pp. 397-399, 1986.

[24]   S. B. Tennakoon, V. V. N. Murthy, and A. Eiumnoh, "Estimation of cropped area and grain yield of rice using remote sensing data," *International Journal of Remote Sensing*, vol. 13, no. 3, pp. 427-439, 1992.

[25]   N. Vassilas, S. Perantonis, E. Charou, S. Varoufakis, and M. Moutsoulas, (1995), "Neural networks for fast and efficient classification of multispectral remote sensing data," [Online] 5th Hellenic Conference on Informatics, Athens, Greece. Available: http://www.sena.gr/epy/11/www/epi95.htm.

[26] T. A. Warner and M. Shank, "An evaluation of the potential for fuzzy classification of multispectral data using artificial neural networks," *Photogrammetic Engineering and Remote Sensing*, vol. 63, no. 11, pp. 1285-1294, November, 1997.

[27] T. Wassenaar, F. Baret, J. Robbez-Masson, and P. Andrieux, "Sunlit soil surface extraction from remotely sensed imagery of perennial, discontinuous crop areas; the case of Mediterranean vineyards," *Agronomie*, vol. 21, pp. 235-245, 2001.

[28] J. S. Weszka, C. R. Dyer, and A. Rosenfeld, "A comparative study of texture measures for terrain classification," *IEEE Transactions on System, Man, and Cybernetics*, vol. SMC-6, no. 4, pp. 269-285, April, 1976.

[29] T. Yoshida and S. Omatu, "Neural network approach to land cover mapping," *IEEE Transactions on Geoscience and Remote Sensing*, vol. 32, no. 5, pp. 1103-1109, September, 1994.

[30] J. Zhang and G. M. Foody, "Fully-fuzzy supervised classification of sub-urban land cover from remotely sensed imagery: statistical and artificial neural network approaches," *International Journal Of Remote Sensing*, vol. 22, no. 4, pp. 615-628, 2001.

TABLE 2.1
COMPARISON OF THE PRODUCER'S ACCURACY (%) FOR ANALYSIS BASED ON VARIOUS
NUMBER OF HISTOGRAM CELLS

	HISTOGRAM CELL		
Class	64	128	256
City	96	100	98
Forest	98	96	98
Dark field	64	70	68
Medium dark field	94	98	98
Light field	98	98	96
Water	84	78	72
Overall accuracy (%)	89	90	88

TABLE 2.2
ERROR MATRIX FOR THE EVALUATION DATA SET OF THE NEURAL NETWORK BASED ON THE
HISTOGRAM APPROACH

	Reference Data						
Class	City	Forest	Dark field	Medium dark field	Light field	Water	Total
City	50	0	0	0	1	0	51
Forest	0	48	9	0	0	2	59
Dark field	0	1	35	0	0	6	42
Medium dark field	0	0	1	49	0	3	53
Light field	0	0	0	0	49	0	49
Water	0	1	5	1	0	39	46
Total	50	50	50	50	50	50	300
Producer's Accuracy (%)	100	96	70	98	98	78	90[a]
User's Accuracy (%)	98	81	83	92	100	85	

[a] – Overall accuracy (%)

TABLE 2.3
COMPARISON OF THE PRODUCER'S ACCURACY (%) FOR ANALYSIS BASED ON SPATIAL
INFORMATION OF THE WINDOW

Class	Window Size				
	1x1	3x3	5x5	10x10	15x15
City	36	56	40	18	26
Forest	56	44	58	44	2
Dark field	38	64	46	50	56
Medium dark field	96	68	98	96	76
Light field	84	92	94	100	100
Water	40	72	46	48	72
Overall Accuracy (%)	58	66	64	59	53

TABLE 2.4
ERROR MATRIX FOR THE EVALUATION DATA SET OF THE NEURAL NETWORK BASED ON THE
SPATIAL APPROACH

Class	Reference Data						
	City	Forest	Dark field	Medium dark field	Light field	Water	Total
City	28	0	0	1	2	0	31
Forest	0	22	2	0	0	0	26
Dark field	0	21	32	0	0	7	60
Medium dark field	5	1	2	34	2	7	53
Light field	14	0	0	1	46	0	61
Water	1	6	14	14	0	36	71
Total	50	50	50	50	50	50	300
Producer's Accuracy (%)	56	44	64	68	92	72	*66*[a]
User's Accuracy (%)	90	85	53	67	75	51	

[a] – Overall accuracy (%)

TABLE 2.5
COMPARISON OF THE PRODUCER'S ACCURACY (%) FOR ANALYSIS BASED ON THE
TEXTURAL PARAMETERS OF THE WINDOW

Class	Window Size				
	3x3	5x5	10x10	15x15	Entire image
City	68	64	90	90	98
Forest	88	94	94	88	92
Dark field	50	42	56	62	80
Medium dark field	92	96	90	90	98
Light field	94	96	96	96	98
Water	60	58	60	78	84
Overall Accuracy (%)	75	75	81	84	92

TABLE 2.6
ERROR MATRIX FOR EVALUATION DATA SET OF THE NEURAL NETWORK BASED ON
TEXTURAL APPROACH

Class	Reference Data						
	City	Forest	Dark field	Medium dark field	Light field	Water	Total
City	49	0	0	0	1	1	51
Forest	0	46	6	0	0	1	53
Dark field	0	4	40	0	0	5	49
Medium dark field	0	0	1	49	0	1	51
Light field	1	0	0	0	49	0	50
Water	0	0	3	1	0	42	46
Total	50	50	50	50	50	50	300
Producer's Accuracy (%)	98	92	80	98	98	84	92^a
User's Accuracy (%)	96	87	82	96	98	91	

[a] – Overall accuracy (%)

TABLE 2.7
COMPARISON OF THE PRODUCER'S ACCURACY (%) FOR ANALYSIS BASED ON VARIOUS
COMBINATIONS OF TEXTURAL PARAMETERS

Class	Combination				
	ASM[a] & IDM[b]	Mean & SD[c]	ASM[a] & IDM[b] & Mean	ASM[a] & IDM[b] & SD[c]	All
City	68	94	90	94	98
Forest	52	84	92	86	92
Dark field	40	68	78	54	80
Medium dark field	26	84	94	52	98
Light field	32	96	98	72	98
Water	36	64	82	72	84
Overall Accuracy (%)	58	82	89	72	92

[a] – Angular second moment
[b] – Inverse difference moment
[c] – Standard deviation

TABLE 2.8
COMPARISON OF THE PRODUCER'S ACCURACY (%) FOR ANALYSIS BASED ON VARIOUS
COMBINATIONS OF THE HISTOGRAM TEXTURAL AND SPATIAL APPROACHES

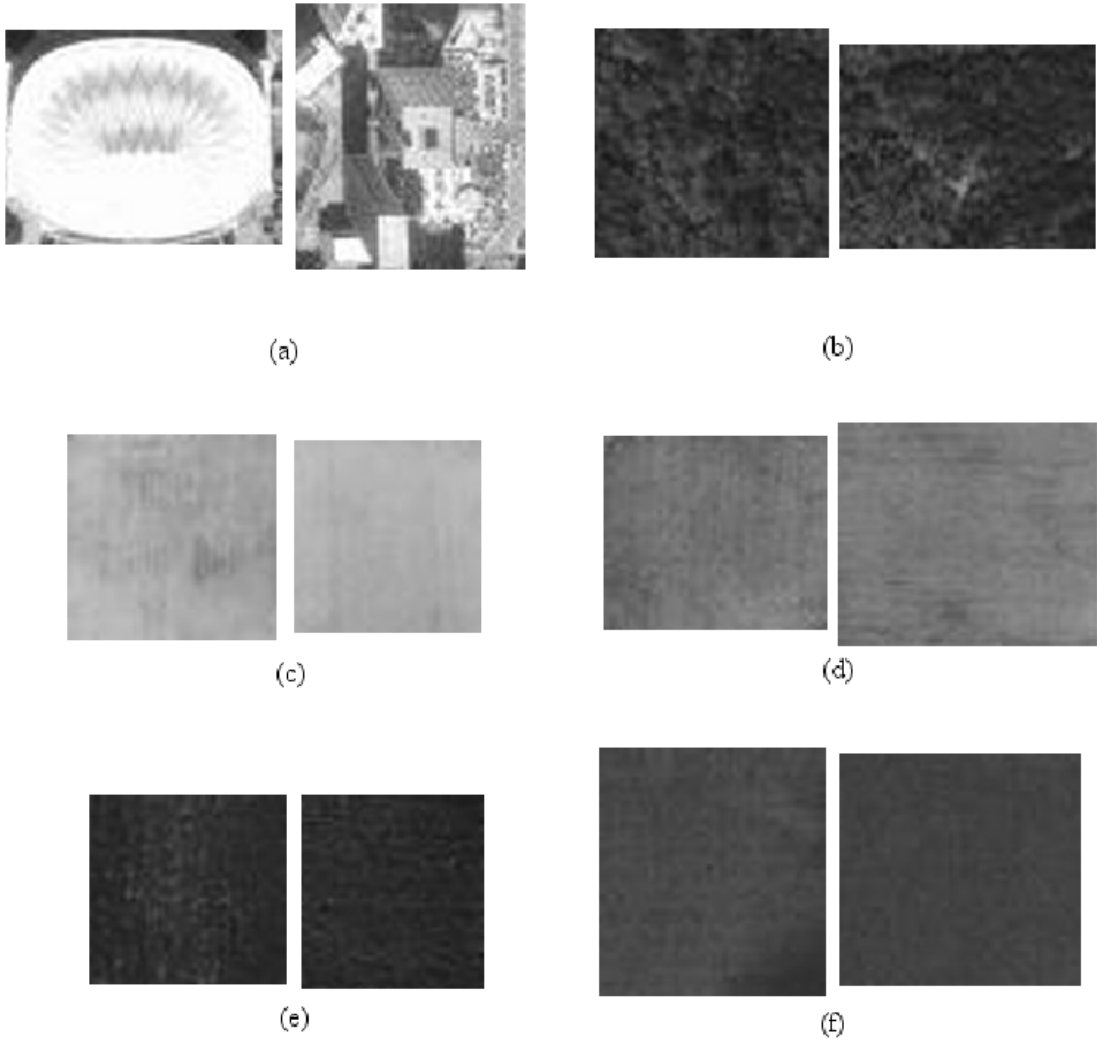| Class	Combination				
	Histogram & Textural	Textural & Spatial	Histogram & Spatial	Histogram, Textural & Spatial	Textural
City	100	98	98	96	98
Forest	98	88	94	94	92
Dark field	54	76	64	66	80
Medium dark field	96	96	98	98	98
Light field	98	100	98	98	98
Water	80	70	82	92	84
Overall Accuracy (%)	88	88	89	89	92
Std. Dev.	18	12	14	12	8

Fig. 1.1. Examples of different land-use classes. (a) city, (b) forest, (c) light field, (d) medium dark field, (e) dark field, (f) water.
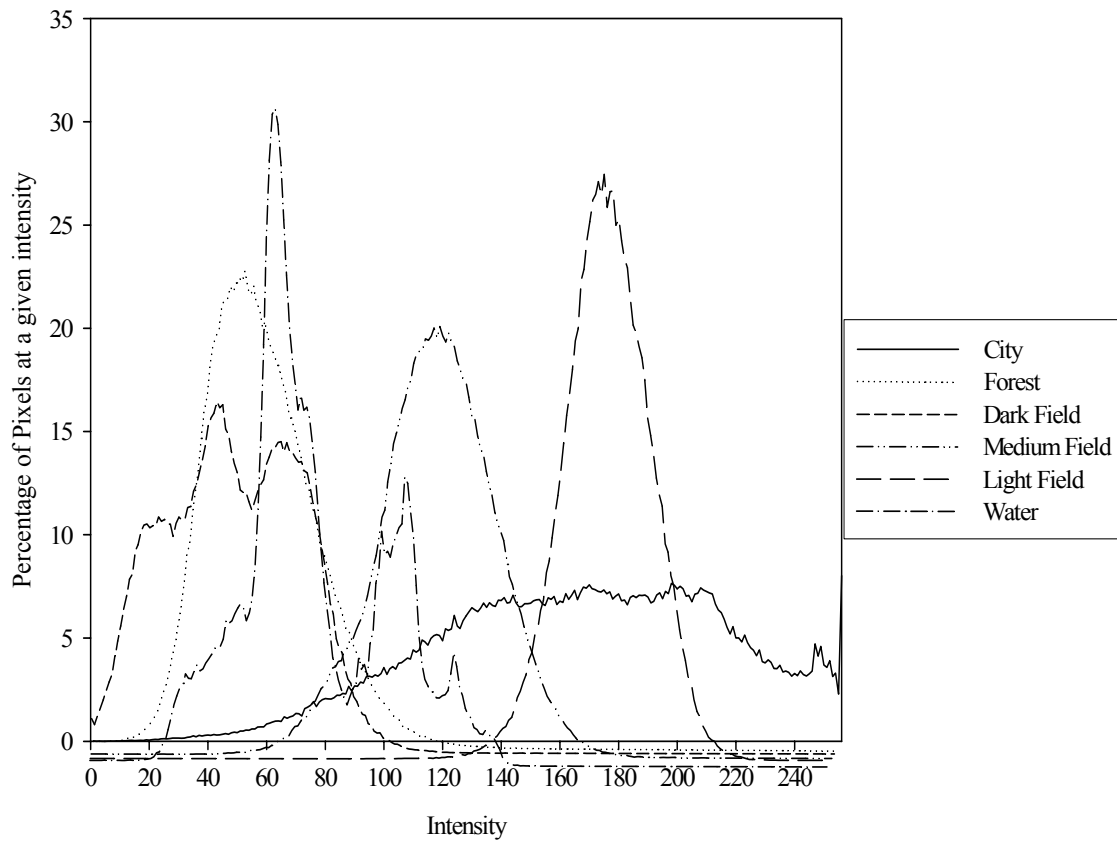
Fig. 1.2. Normalized histogram of intensities for each class.

CHAPTER 3

LAND-USE CLASSIFICATION OF MULTISPECTRAL AERIAL IMAGES USING

ARTIFICIAL NEURAL NETWORKS[2]

Abstract—During the past decade, there have been significant improvements in remote sensing technologies, which have provided high-resolution data at shorter time intervals. Considerable effort has been directed toward developing new classification strategies for analyzing this imagery. The goal of this study was to develop an Artificial Neural Network (ANN) based technique for the classification of multispectral aerial images for land-use in agricultural and environmental applications. The specific land-use classes included water, forest, and several different types of agricultural fields. Three approaches were used for the preparation of the inputs to the ANN. These included histograms of the pixel intensities, textural parameters extracted from the image, and matrices of the pixels for spatial information. A probabilistic neural network was employed. Seven hundred images were used for model development and 175 for independent model evaluation. The overall accuracy for the evaluation data set was 74% for the histogram approach, 71% for the spatial approach and 89% for the textural approach. The evaluation of ANNs based on various combinations of all three approaches did not show an improvement in accuracy. We also found that some approaches can be used selectively for certain classes. For example, the textural approach worked best for forest classes. For future studies, edge detection prior to classification with more careful selection of each class should be included for land use classification of multispectral images.

3.1. Introduction

Remote sensing and image classification

Remote sensing technology is currently being used to obtain and interpret geo-spatial data employing different radiation spectra. This technology is applicable in developing information about features, objects, and classes for the earth's land surfaces, oceans, and atmosphere. With the recent advances in remote sensing, high-resolution data are available at shorter time intervals. For example, the Landsat 7 satellite operated by the United States Geological Survey (USGS) can provide remote sensing data in a 16-day repeat cycle from a panchromatic band with 15-meter spatial resolution (Short, 1999). The SPOT 5 satellite has up to a 2.5-meter ground resolution in panchromatic mode with a 26-day repeat cycle (Short, 1999). However, aerial images can achieve even higher resolutions, depending on the type of sensor that is being used. The cost of high-resolution images has become comparatively low and images are more readily available due to advances in sensing techniques and commercialization of many of these technologies.

Another major advancement in remote sensing has been in the field of imaging spectroscopy. Remote sensors that cover two thermal intervals corresponding to two atmospheric windows allow sensing of thermal emissions from land, water, ice and the atmosphere. These sensors have been flown on airplanes for several decades. Many of the meteorological satellites include at least one thermal channel along with other sensors. A thermal band has also been included on the Landsat Thematic Mapper. Radar systems are another class of satellite remote sensors that are currently operational in space. Radar normally provides a very different view of the same landscape compared to a visible

image because of its ability (for certain wavelengths) to penetrate clouds. Seasat, the Spaceborne Imaging Radar (SIR) series, and Radarsat are among the instruments used so far. The Multispectral Scanner (MSS) has been the most important sensor and was part of the first five Landsats. The Landsat MSS gathers radiation over spectral bandwidths that integrate radiation over relatively broad intervals (0.1 and 0.3 μm). Thus, instead of the spectral signatures that continuously measure spectral response in very narrow intervals, the MSS data when plotted produce histogram-like bars that are rough approximations of the signature curves. Hyperspectral imaging is a powerful and versatile means for continuous sampling of broad intervals of the spectrum. Hyperspectral imaging allows a sensor on a moving platform to gather reflected radiation from a ground target such that a special detector system can record up to 217 spectral channels (each approximately 10 nanometers in width) simultaneously over the range from 0.38 to 2.5 mm. With such detail, the ability to detect and identify individual materials or classes greatly improves.

Image classification is a key component of remote sensing (Baraldi and Parmiggiani, 1990; Biscoff et al., 1992; Carmel and Kadmon 1998; Mukherjee 2002). Image classification is the process of creating thematic maps from satellite imagery. A thematic map is an informational representation of an image, which shows the spatial distribution of a particular theme. An example of themes could be vegetation types consisting of trees, crops, and grasslands. Finer sub-themes can also be defined inside a theme to make the process of classification more refined, such as classifying trees as deciduous or evergreen. Image classification relies on the spectral distinctness of classes or spectro-temporal variability. It also depends on the context of classification. For example, two features with nearly identical spectral signatures for vegetation could be assigned to the

34

classes 'forest' and 'crops' depending on whether the area in the image has irregular or straight boundaries. Various studies reported a high accuracy in image classification (Ritter and Hepner, 1990; Chen et al., 1995; Du, 1996; Carmel and Kandmon, 1998; Tsai, 2002). However, it is vital to extend techniques to further improve remote sensing image classification accuracy for deriving dependable land cover information for vegetation, land-use and other applications.

Most land-use classes have a characteristic value for intensity, which is used in generating spectral classes from image classification. The spatial composition of these spectral classes within a certain spatial range can be useful information for image classification (Fung and Chan, 1994). Images can also be classified based on texture information from the image. Several parameters related to the texture recognition of an image were proposed by Haralick (1973). These include angular second moment, contrast, correlation, inverse difference moment, and entropy. Angular second moment is a measure of the homogeneity of the image. Contrast is a measure of the amount of local variation present in an image. Correlation is a measure of gray-tone linear-dependencies in the image. Inverse difference moment is a measure of the amount of local similarity. Entropy is a measure of the average uncertainty of gray tone co-occurrence in the image. Contrast, entropy, angular second moment and inverse difference moment have been widely used for image classification and image analysis. Jensen (1979) applied these Haralick's measures to Landsat images for land cover classification and achieved up to 80% accuracy. Marceau et al. (1990) used the same Haralick's textural parameters for land-cover classification of nine land-cover types in SPOT imagery and achieved up to 100% accuracy for some land-cover types. Kondo et al. (2000) used the Haralick's

parameters for evaluating sugar and acid content of *Iyokan* orange fruit based on a machine vision system. Singh and Singh (2001) compared several texture methods for image analysis. The performance evaluation was based on the ability of a classifier to recognize unseen samples of the four classes on the basis of training data. The best overall result using nearest neighbour methods was obtained with Haralick's parameters based on co-occurrence matrices.

Artificial neural networks and image classification

Artificial neural networks (ANNs) are computational mathematical models that emulate some of the observed properties of biological neural systems and draw on the analogies of adaptive biological learning. An ANN is composed of a number of interconnected processing elements that are similar to neurons. These processing elements are joined by weighted connections that are analogous to synapses in the human brain. Supervised learning in an ANN typically occurs by example through training or exposure to a known set of input and corresponding output data. The training algorithm adjusts the connection weights through an iterative procedure in which the error is minimized. The superiority of ANNs to some of the classical statistical methods in various problems, including classification problems, has been shown in previous studies (Bischof et al., 1990; Paola and Schowengerdt, 1995; Blackard and Dean, 1999; Giraudel, 2001). ANNs are commonly used for segmentation and classification purposes and are recommended for problems where data diversity is large (Lee et al., 1990; Warner and Shank, 1997; Moshou, 2001).

The viability of land-use classification of remotely sensed image areas with ANNs was established by Benediktsson et al. (1990). Subsequent studies that examined the neural network classifier method in more detail also compared it to standard statistical classification techniques (Paola and Schowengerdt, 1995; Luo et al., 1999; Zhang, 2001). These studies presented several classification approaches that are based on ANNs, such as the pixel-by-pixel or per-pixel method (Salu and Tilton, 1993). The pixel-by-pixel method deals with classification of pixels. The classification aims at attributing each pixel to its correct land cover category. The dimensions of pixels are usually related to the field of view of the sensor that obtained the image, and the sampling rate of the analogue-to-digital converter used to translate the signal received at the detector. It is hypothesized that the statistical characteristics of a group of pixels can be used to define a decision rule for discrimination between the cover type of that pixel and all others. However, this approach faces several difficulties due to the interaction between light and the components of atmosphere and due to the geometry of the imaging system (Mather, 1990). The per pixel method is also not appropriate for classification of high-resolution images because the spatial variability of surface features increases with the increase in spatial resolution (Marceau et al., 1990). Higher variability diminishes classification accuracies (Irons et al., 1985).

There have been several new approaches to classification, such as the contextual classification scheme and methods based on fuzzy sets or their combinations, which have had better success than the more common methods. Contextual classifiers increase the dimensionality of data with additional bands in which contextual information is present in some way or assume the existence of local properties defined on a neighborhood where

37

the spatial dependence is relevant. The fuzzy approach, proposed by Wang (1990), allows for multiple and partial classification of mixed pixels. This approach gives more information on the relative strengths of class membership at the pixel level. Gong and Howarth (1992) found that the contextual classification for land-use classification of SPOT HRV data was better than the conventional maximum likelihood classification method. Cortijo and De la Blanca (1998) achieved 91% accuracy with contextual classification. Papin (2002) demonstrated the accuracy and efficiency of the contextual approach. Gopal and Woodcock (1994) successfully used fuzzy sets for accuracy assessment of thematic maps. Zhang and Foody (2001) used fully-fuzzy supervised classification to determine land cover based on images obtained with Landsat Thematic Mapper and obtained better results than partially-fuzzy classification.

Ashish (2002) developed an ANN based technique for the classification of gray-scale aerial images into various types of land-use classes including city, water, forest and various types of agricultural field areas. Gray-scale aerial images with a 6.5-meter resolution for nine counties were obtained. Three approaches were used for the preparation of the inputs to the ANN, including histograms of the pixel intensities, textural parameters extracted from the image, and matrices of pixels for spatial information. A probabilistic neural network was used in that study. The best ANN was based on textural parameters and achieved an overall accuracy of 92% for the evaluation data set.

The goal of this study was to enhance the scope of the technique developed by Ashish (2002) and to evaluate it for multispectral aerial images for improving agricultural production decision support and policymaking. Specific objectives included the

comparison of different preprocessing approaches using artificial neural networks for the classification of multispectral image for agricultural and environmental land use.

3.2. Materials and methods

Multispectral aerial images at a 1-meter resolution were obtained from the Georgia Geographic Information Systems (GIS) Data Clearinghouse. We used images from the Luthersville quadrangle, located in Meriwether County, Georgia, and from the Sharpsburg quadrangle, located in Coweta County, Georgia. These high-resolution multispectral aerial images were taken in January 1999 and they have been georeferenced and geocorrected. They are commonly known as Digital Orthophotography Quarter-Quadrangles (DOQQs) and the 1999 DOQQs are scanned images of color-infrared aerial photographs. The film that was used for the color-infrared aerial photographs detects several bands of visible light including green, red and near-infrared radiation reflected by healthy vegetation, e.g. chlorophyll in plants. Lush green areas appear red on this imagery and are commonly known as a false color composite image.

We manually selected small subareas of known classes, referred to as "images" herein, from the DOQQs using the software Paintshop Pro (version 6.00). Due to the selection process, images had different sizes. These images were visually separated into seven different classes, including pine forest, hardwood forest, dark agricultural field, medium dark agricultural field, light field with no crop, fallow and water. One hundred twenty five images were obtained for each class making a total of 875 images. Out of the 125 images from each class, 100 were used for model development. The remaining 25 images were kept separately and used as an independent data set for final model evaluation to

determine the overall accuracy of the ANN model. In the model development dataset 80 images were used for training and 20 images for testing. The training set consisted of patterns used to adjust the weights to minimize the error and the test set was used periodically in a feed-forward mode only to determine when to stop training to avoid overfitting. Once the training was completed, the evaluation set was used to assess the accuracy of the model.

The pine and hardwood forest classes are easily distinguishable from each other because the aerial imagery was obtained in January. Hardwood trees do not have any leaves in winter, as all leaves are abscised during the fall, while pine trees keep their needles during the winter. Therefore, the image from a pine forest has a higher infrared content than an image from a hardwood forest. The fallow field areas consisted of fields that contained stubble from the previous crop. The dark field class consisted of images of lush vegetation areas, whereas the medium dark field class consisted of images of relatively less vegetation areas. The light field class consisted of images of uncropped areas. The water class images were obtained from ponds and lakes in the vicinity of fields.

In the first approach for preparing data for input to the ANN, three histograms of pixel intensities were created from the collection of red, green and blue pixel values of the image. They were then normalized based on the number of pixels from the entire image to allow a comparison of images of different sizes. Various cell widths were also considered to determine the effect on accuracy. For the second approach, the spatial information of an image was extracted from the central part of the image. This spatial information corresponded to the intensity of the red, green and blue pixels in the specific

spatial order to preserve their relative location in the grid. The central portion of the image used for extracting preprocessed information is termed as "window" herein. The window sizes used for the spatial approach were 1x1, 3x3, 5x5, 11x11, and 15x15 pixels. In the third approach, textural parameters were calculated from pixel data of either the entire image or the "window" of the image according to the different techniques proposed by Haralick (1973). Three sets of the textural parameters were calculated based on the red, green and blue pixels. The textural parameters used in this study were angular second moment (ASM), inverse difference moment (IDM), contrast and entropy.

$$ASM = \sum_i \sum_j \{p(i,j)\}^2 \qquad (1)$$

$$IDM = \sum_i \sum_j \frac{1}{1+(i-j)^2} p(i,j) \qquad (2)$$

$$Contrast = \sum_i \sum_j (i-j)^2 p(i,j) \qquad (3)$$

$$Entropy = -\sum_i \sum_j p(i,j) \log(p(i,j)) \qquad (4)$$

where $p(i,j)$ is a value in co-occurrence matrix which represents the number of times pixel a has a value i and pixel b has value j when pixel a is a neighbor of pixel b, a and b varying over the entire image. These are the most frequently used parameters (Carlson, 1995; Singh et al., 2000, Franklin, 2001) and found to have the best performance among textural parameters (Conners and Harlow, 1980; Du Buf et al. 1990; Singh and Singh, 2001). In addition, the mean and standard deviation (SD) of pixel intensities were also used with Haralick's textural parameters. The window sizes that were analyzed included 3x3, 5x5, 7x7, 11x11, 15x15, 17x17, 19x19 and 21x21 pixels and the entire image. The

size of the window was limited to a maximum of 21x21 pixels because of the size of the images that were extracted.

After preprocessing, the data were presented to an ANN for training. The software Neuroshell 2 (release 3, Ward System Group Inc.) was used in this study. In preliminary tests, the Probabilistic Neural Network (PNN) (Specht, 1990) was found to have a higher accuracy than the standard back propagation algorithm and was therefore used for all subsequent model development. In a PNN, the number of hidden layer neurons is equal to the number of patterns in the training set and the output layer has the same number of neurons as the number of classes. The PNN output for each node generally corresponds to the probability that the pattern should be considered in that class. A Gaussian activation function is used for the output nodes.

The best ANN was selected based on the highest overall accuracy of the evaluation data set. Overall accuracy is a function of the performance of the ANN on the combined classes, which was calculated from the error matrix of the classification results (Story and Congalton, 1986). Overall accuracy is the ratio of the sum of correctly classified patterns of all classes over the total number of patterns presented to the ANN. The error matrix can also provide information about the producer's and user's accuracy. The producer's accuracy is the ratio of the number of correctly classified patterns of a class over the total number of patterns of that class presented to the network. The user's accuracy is the ratio of number of correctly classified patterns into a class over the total number of patterns classified as being in that class.

Using the same data sets, each of the three approaches for preparing input data was considered individually. In the textural approach, there were four different parameters per

42

spectrum used as input for textural information. A separate study was conducted to determine if the same level of accuracy could be attained if one or more of the inputs were eliminated. After testing all three approaches individually, a study was conducted considering various combinations of approaches in order to determine if the accuracy could be further improved.

3.3.   Results and discussion

Histogram

A comparative study was conducted for the ANN development based on inputs of histograms of 32, 64, 128 and 256-cells (Table 3.1). The overall accuracy of 32-cells histogram was 71%. The 64-cell network had an overall accuracy of 74%, which was highest among all the cases considered. The overall accuracy of 128-cells histogram was 72% and overall accuracy of 256-cells histogram was 73%. The fallow class had the lowest producer's accuracy (32%) for all histograms. The producer's accuracy of the dark field and the medium dark field classes decreased with an increasing number of histogram cells past the 64-cell histogram. For the 64-cell histogram, 17 of the 25 images of the fallow class were misclassified into the hardwood forest class (Table 3.2). The water class also showed a low producer's accuracy (48%). This could be attributed to the high variation in the color of water images, including light and dark blue, green and even images that were somewhat reddish in color. Misclassification of field classes, including dark, medium dark and light field, was only among other field classes. The classification of the pine and hardwood forest classes was most accurate, with a 100% producer's accuracy. The comparison of the user's accuracy for the evaluation data set showed that

43

the fallow class had the lowest user's accuracy (57%) with only eight out of 14 images correctly classified as fallow, while six water images were misclassified as fallow. The hardwood forest class also had a low user's accuracy (60%) due to misclassification of 17 fallow images as hardwood forest image. The dark field and medium dark field classes had low user's accuracy (60% and 64%, respectively) mainly due to misclassification of images of one field class into other field classes. The pine forest and the water classes had the highest user's accuracies (100%), followed by the light field class (96%) (Table 3.2).

Spatial

   The effect of various window sizes of the spatial matrix presented to the network was examined. The ANNs based on the 5x5, 7x7 and 11x11 pixel window resulted in the highest overall accuracy of 71% (Table 3.3). The ANNs classified 124 patterns out of a total of 175 patterns correctly. The 5x5 and 7x7 window size performed the best (76%) for the dark field class. The 7x7 and 11x11 window sizes performed the best (100%) for the medium dark field class and the 5x5 and 11x11 window sizes performed the best for light field (76%) and water (72%) classes. Overall, based on the individual classification categories, the 5x5 window size had the best performance, as the producer's accuracy for five, i.e. dark field, light field, pine forest, hardwood forest and water, out of seven classes was the best among the three window sizes (5x5, 7x7, and 11x11). The two classes for which the 5x5 window size performed less than the best window size (11x11 window) were the medium dark field and the fallow classes. In case of the 7x7 window network, the producer's accuracy for two, i.e. dark field and medium dark field, out of

seven classes was the best. In case of the 11x11 window network the producer's accuracy for four, i.e. medium dark field, light field, fallow and water, out of seven classes was the best. The standard deviation of the producer's accuracies for different classes for the 5x5 window network ANN was the smallest (18%), which further shows the consistently good performance of the 5x5 window size ANN. The images of fallow and hardwood forest classes were misclassified among each other. Eleven fallow images were misclassified as hardwood forest and 11 hardwood forest images were misclassified as fallow (Table 3.4). This was one of the reasons that fallow and hardwood forest classes had the smallest producer's accuracies, i.e. 48% and 44%, respectively, and the smallest user's accuracies, i.e. 40% and 50%, respectively. Seven of the water images were also misclassified as fallow. Similar to the histogram approach, the misclassification of field classes, including dark, medium dark and light field, was only into other field classes. Three of the pine forest images were also misclassified as field images: two as dark field and one as medium dark field. Two hardwood forest images were misclassified as light field. The cause for misclassification of forest areas, including pine and hardwood forests into field areas, could be due to less spatial variation in the central window of these images compared to other classes.

Textural

The overall accuracy of the ANNs based on the six textural parameters for the window sizes 3x3 to 21x21 ranged from 72% to 89% (Table 3.5). The six textural parameters for the 21x21 window performed best among all window sizes for the textural approach. The overall accuracy for the six textural parameters of the 21x21 window ANN was 89%. The

overall accuracy for the entire image was 79%. The performance of the 21x21 window network for classes with more evident texture, including fallow, pine forest and hardwood forest was good, with producer's accuracies of 80%, 100% and 100%, respectively. The ANNs based on textural parameters for field classes, including dark, medium dark, and light field performed slightly lower with producer's accuracies of 88%, 84%, and 88%, respectively (Table 3.6). This lower performance may be attributed to the lack of significant texture in these images. For example, the average value of inverse difference moment of red pixels for dark field class was 0.09, whereas that for pine forest was 0.03 (Table 3.7). Inverse difference moment is the measure of local similarity. The higher value of inverse difference moment shows more similarity of pixels and less significant texture.

When one or more of the textural parameters were eliminated, the overall accuracy of the 21x21 window ANN was reduced (Table 3.8). This indicated that all textural parameters were important as input parameters for the classification process. The ANN based on the combination of five parameters, excluding standard deviation of pixel intensities, had an overall accuracy of 86%. The ANN based on the combination of five parameters, excluding the mean of pixel intensities, had an overall accuracy of 79%. The overall accuracy of the ANN based on the combinations of five parameters was 76% when contrast was excluded and 79% when entropy was excluded. The ANN based on a combination of four Haralick's parameters, by excluding the mean and standard deviation of pixel intensities, had an overall accuracy of 80%. The combination of four parameters, including ASM, IDM, mean and standard deviation of pixel intensities, had overall

accuracy of 83%. Therefore, the best overall accuracy was for the ANN including all six textural parameters for each of the three spectra.

Combinations of Histogram, Spatial and Textural information

The overall accuracy of the ANN based on the textural approach did not improve by using ANNs based on combinations of histogram, spatial and textural information (Table 3.9). In these tests, the ANN with the combination of histogram, textural and spatial data had an overall accuracy of 71% and the standard deviation of the producer's accuracies was 21%. The ANN based on the combination of histogram and spatial approach had an overall accuracy of 69% and the standard deviation of the producer's accuracies was 25%. The ANN based on the combination of histogram and textural approach had an accuracy of 74% and the standard deviation of the producer's accuracies was 26%. The ANN based on the combination of textural and spatial approach performed the best when considering the various combinations of ANNs (79%). The standard deviation of the producer's accuracies was also the smallest for the ANN based on textural and spatial approach (9%), which indicated that the results were more consistent.

The ANN based solely on textural parameters had the highest overall accuracy of 89% for the evaluation data set. It also had the smallest standard deviation (8%) for the producer's accuracy. An overall accuracy of 89% for the classification of multispectral images using ANNs for land-use was similar to previous observations (Yoshida and Omatu, 1994; Paola and Schowengerdt, 1995). The improved performance of the textural approach compared to other approaches in our study on multispectral images is also consistent with the results of previous studies based on textural approaches on gray-scale

and multispectral images. (Weszka et al., 1976; Marceau et al., 1990; Singh and Singh, 2001).

The output of each of the seven nodes of the PNN was averaged over the 25 patterns in the evaluation dataset. These values are shown in Table 3.10. When the average value for another node was 0.02 or greater, it is also shown under misclassification. This gives an indication when the PNN is uncertain of the correct classification. A plot of producer's accuracy versus average network output for the 25 patterns in the evaluation dataset is shown in Figure 3.1. The coordinate values of each data point are shown in parenthesis by each plotted point. The PNN output thus provides an indication of the certainty of the classification of an image.

3.4. Summary and conclusions

In this study, three different approaches to preparing inputs to ANNs for image classification based on ANNs were evaluated. All three approaches were tested useing a range of window sizes. Good results were obtained using textural parameters for an ANN-based classification methodology of aerial multispectral images for seven land-use classes, including water, forest, and several different types of agricultural fields. The best ANN from each approach was also used in combination to test the performance for image classification. The results showed that the textural approach using Haralick's parameters based on co-occurrence matrix and mean and standard deviation of pixel intensities had the highest accuracy. The overall accuracy did not improve by using ANNs based on combinations of histogram, spatial and textural information. It was also found that larger window sizes for textural parameters helped in improving the results. The best results

were obtained using 21x21 window size for textural parameters. The highest overall accuracy of 89% was achieved for an ANN based on the textural parameters for classification, compared to approaches based on histogram and spatial information. This study further established the importance of the use of textural parameters for the classification of remotely sensed images. The misclassification of field areas and water into one another can possibly be solved with the help of a histogram analysis, as the histogram approach showed good results for these three classes. Edge detection prior to classification can help automate the process of image selection.

3.5. Acknowledgements

References

Ashish, D., 2002. Land-use classification of aerial images using artificial neural networks, M.S. Thesis, Artificial Intelligence, University of Georgia, Athens, U.S.A.

Baraldi, A., and Parmiggiani, F., 1990. Urban area classification by mulitspectral SPOT images, IEEE Trans. Geosci. Remote Sensing 28 (4), 674-680.

Benediktsson, J. A., Swain, P. H., and Ersoy, O. K., 1990. Neural network approaches versus statistical methods in classification of multisource remote sensing data, IEEE Trans. Geosci. Remote Sensing 28 (4), 540-551.

Bischof, H., Schneider, W., and Pinz, A. J., 1992. Multispectral classification of Landsat-images using neural networks, IEEE Trans. Geosci. Remote Sensing 30 (3), 482-490.

Blackard, J. A., and Dean, D. J., 1999. Comparative accuracies of artificial neural networks and discriminant analysis in predicting forest cover types from cartographic variables, Comput. Electron. Agric. 24, 131-151.

Carlson, G. E., 1995. Cooccurrence matrices for small region texture measurement and comparison, Int. J. Remote Sensing 16 (8), 1417-1423.

Carmel, Y., and Kadmon, R., 1998. Computerized classification of Mediterranean vegetation using panchromatic aerial photographs, Journal of Vegetation Science 9 (3), 445-454.

Chen, Y. Q., Nixon, M. S., and Thomas, D. W., 1995. Statistical geometrical features for texture classification, Pattern Recognition 28 (4), 537-552.

Conners, R. W., and Harlow, C. A., 1980. A theoretical comparison of textural algorithms, IEEE Trans. Pattern Anal. Machine Intell. 2 (3), 204-222.

Cortijo, F. J. and De la Blanca, N. P., 1998. Improving classical contextual classifications, Int. J. Remote Sensing 19 (8), 1591-1613.

Du, L., 1996. Fuzzy classification of earth terrain covers using complex polarimetric SAR data, Int. J. Remote Sensing 17 (4), 809-826.

Du Buf, J. M. H., Kardan, M., and Spann, M., 1990. Texture feature performance for image segmentation, Pattern Recognition 23 (3/4), 291-309.

Franklin, S. E., 2001. Using spatial co-occurrence texture to increase forest structure and species composition classification accuracy, Photogramm. Eng. Remote Sens. 67 (7), 849-855.

Fung, T. and Chan, K., 1994. Spatial composition of spectral classes: a structural approach for image analysis of heterogeneous land-use and land-cover types, Photogramm. Eng. Remote Sens. 60 (2), 173-180.

Giraudel, J. L., 2001. A comparison of self-organizing map algorithm and some conventional statistical methods for ecological community ordination, Ecological Modelling 146 (1-3), 329-339.

Gong, P. and Howarth, P. J., 1992. Frequency based contextual classification and gray-level vector reduction for land-use identification, Photogramm. Eng. Remote Sens. 58 (4), 423-437.

Gopal, S. and Woodcock, C., 1994. Theory and methods for accuracy assessment of thematic maps using fuzzy sets, Photogramm. Eng. Remote Sens. 60 (2), 181-188.

Haralick, R. M., Shanmugam, K., and Dinstein, I., 1973. Textural features for image classification, IEEE Trans. Syst., Man, and Cybern. 3 (6), 610-621.

Irons, J. R. Markham, B. L., Nelson, R. F., Toll, D. L., Williams, D. L., Latty, R. S., Stauffer, M. L., 1985. The effect of spatial resolution on the classification of Thematic Mapper data, Int. J. Remote Sensing 6 (8), 1385-1403.

Jensen, J. R., 1979. Spectral and textural features to classify elusive land cover at the urban fringe, Professional Geographer 31 (4), 400-409.

Kondo, N., Ahmad, U., Monta, M., and Murase, H., 2000. Machine vision based quality evaluation of Iyokan orange fruit using neural networks, Comput. Electron. Agric. 29, 135-147.

Lee, J., Weger, R. C., Sengupta, S. K., and Welch, R. M., 1990. A neural network approach to cloud classification, IEEE Trans. Geosci. Remote Sensing 28 (5), 846-855.

Luo, X., Jayas, D. S., and Symons, S. J., 1999. Comparison of statistical and neural network methods for classifying cereal grains using machine vision, Trans. of the ASAE 42 (2), 413-419.

Marceau, D. J., Howarth, P. J., Dubois, J. M., and Gratton, D. J., 1990. Evaluation of the gray-level co-occurrence matrix method for land cover classification using SPOT imagery, IEEE Trans. Geosci. Remote Sensing 28 (4), 513-519.

Mather, P. M., 1990. Theoretical problems in image classification, In: Clark, J. A. and Sevens, M. D. (Eds.), Application of Remote Sensing in Agriculture, London, Butterworths, pp. 127-135.

Moshou, D., Vrindts, E., De Ketelaere, B., De Baerdemaeker, J., and Ramon, H., 2001. A neural network based plant classifier, Comput. Electron. Agric. 31 (1), 5-16.

Paola, J. D. and Schowengerdt, R. A., 1995. A detailed comparison of neural network and maximum likelihood classifiers for urban land use classification, IEEE Trans. Geosci. Remote Sensing 33 (4), 981-996.

Papin, C., 2002. Unsupervised segmentation of low clouds from infrared METEOSAT images based on a contextual spatio-temporal labeling approach, IEEE Trans. Geosci. Remote Sensing 40 (1), 104-114.

Ritter, N. D. and Hepner, G. F., 1990. Application of an artificial neural network to land-cover classification of thematic mapper imagery, Computers and Geosciences 16 (6), 873-880.

Salu, Y. and Tilton, J., 1993. Classification of multispectral image data by the binary

diamond neural network and by nonparametric, pixel-by-pixel methods, IEEE Trans.

Geosci. Remote Sensing 31 (3), 606-617.

Short, N. M., 1999. Remote sensing tutorial, Available Online:

http://rst.gsfc.nasa.gov/start.html.

Singh, M. and Singh, S., 2001. Evaluation of texture methods for image analysis," Proc.

7th Australian and New Zealand Intelligent Information Systems Conference (18-21

November, 2001), Perth, Australia, pp. 117-121.

Singh, S., Markou, M. and Haddon, J. F., 2000. Natural object classification using

artificial neural networks, Proc. IEEE International Joint Conference on Neural

Networks (24-27 July, 2000), Como, Italy, IEEE Press, vol. 3, pp. 139-144.

Specht, D. F., 1990. Probabilistic neural network, Neural Networks 3 (1), 109-118.

Story, M. and Congalton, R. G., 1986. Accuracy assessment: a user's perspective,

Photogramm. Eng. Remote Sens. 52 (3), 397-399.

Tsai, F., 2002. A derivative-aided hyperspectral image analysis system for land-cover

classification. IEEE Trans. Geosci. Remote Sensing 40 (2), 416-425.

Wang, F., 1990. Fuzzy Supervised Classification of Remote Sensing Images, IEEE

Trans. Geosci. Remote Sensing 28 (2), 194-201.

Warner, T. A. and Shank, M., 1997. An evaluation of the potential for fuzzy

classification of multispectral data using artificial neural networks, Photogramm. Eng.

Remote Sens. 63 (11), 1285-1294.

Weszka, J. S., Dyer C. R., and Rosenfeld, A., 1976. A comparative study of texture measures for terrain classification, IEEE Trans. Syst., Man, and Cybern. 6 (4), 269-285.

Yoshida, T. and Omatu, S., 1994. Neural network approach to land cover mapping, IEEE Trans. Geosci. Remote Sensing 32 (5), 1103-1109.

Zhang, J. and Foody, G. M., 2001. Fully-fuzzy supervised classification of sub-urban land cover from remotely sensed imagery: statistical and artificial neural network approaches, Int. J. Remote Sensing 22 (4), 615-628.

TABLE 3.1

COMPARISON OF THE PRODUCER'S ACCURACY (%) FOR ANALYSIS BASED ON THE NUMBER OF HISTOGRAM CELLS

	Histogram cells			
	32	64	128	256
Class				
Dark field	40	60	52	48
Medium dark field	84	84	80	76
Light field	80	92	96	96
Fallow	32	32	32	32
Pine forest	100	100	100	100
Hardwood forest	100	100	100	100
Water	60	48	44	60
Overall accuracy	71	74	72	73
Standard Deviation	28	27	29	27

TABLE 3.2

ERROR MATRIX FOR THE EVALUATION DATA SET OF THE NEURAL NETWORK BASED ON THE 64-CELLS HISTOGRAM APPROACH

	Reference Data							
	Dark field	Medium dark field	Light field	Fallow	Pine forest	Hardwood forest	Water	Total
Dark field	15	4	0	0	0	0	6	25
Medium dark field	10	21	2	0	0	0	0	33
Light field	0	0	23	0	0	0	1	24
Fallow	0	0	0	8	0	0	6	14
Pine forest	0	0	0	0	25	0	0	25
Hardwood forest	0	0	0	17	0	25	0	42
Water	0	0	0	0	0	0	12	12
Total	25	25	25	25	25	25	25	175
Producer's accuracy (%)	60	84	92	32	100	100	48	74[a]
User's accuracy (%)	60	64	96	57	100	60	100	

[a] – Overall accuracy (%)

TABLE 3.3
COMPARISON OF THE PRODUCER'S ACCURACY (%) FOR ANALYSIS BASED ON SPATIAL
INFORMATION OF DIFFERENT WINDOW SIZES

	Window Size					
Class	1x1	3x3	5x5	7x7	11x11	15x15
Dark field	72	80	76	76	68	76
Medium dark field	84	63	92	100	100	100
Light field	80	83	76	64	76	88
Fallow	48	47	48	76	84	76
Pine forest	92	92	88	84	76	40
Hardwood forest	60	45	44	28	20	4
Water	40	100	72	68	72	72
Overall accuracy	68	70	71	71	71	65
Standard Deviation	19	22	18	22	25	33

TABLE 3.4
ERROR MATRIX FOR THE EVALUATION DATA SET OF THE NEURAL NETWORK BASED ON THE
5X5 WINDOW SIZE SPATIAL APPROACH

	Reference Data							
	Dark field	Medium dark field	Light field	Fallow	Pine forest	Hardwood forest	Water	Total
Dark field	19	2	0	0	2	0	0	23
Medium dark field	5	23	6	0	1	0	0	35
Light field	1	0	19	1	0	2	0	23
Fallow	0	0	0	12	0	11	7	30
Pine forest	0	0	0	0	22	0	0	22
Hardwood forest	0	0	0	11	0	11	0	22
Water	0	0	0	1	0	1	18	20
Total	25	25	25	25	25	25	25	175
Producer's Accuracy (%)	76	92	76	48	88	44	72	71[a]
User's Accuracy (%)	83	66	83	40	100	50	90	

[a] – Overall accuracy (%)

TABLE 3.5
COMPARISON OF THE PRODUCER'S ACCURACY (%) FOR ANALYSIS BASED ON TEXTURAL
PARAMETERS OF DIFFERENT WINDOW SIZES

	Window Size								
Class	3x3	5x5	7x7	11x11	15x15	17x17	19x19	21x21	Entire image
Dark field	72	64	48	52	76	84	80	88	56
Medium dark field	96	96	96	96	84	84	76	84	72
Light field	64	64	76	60	96	92	92	88	36
Fallow	52	44	76	52	64	64	64	80	88
Pine forest	100	100	100	100	100	100	100	100	100
Hardwood forest	60	76	76	88	92	100	96	100	100
Water	60	68	92	100	88	84	80	80	100
Overall accuracy	72	73	81	78	86	87	84	89	79
Standard Deviation	19	20	18	23	12	12	13	8	25

TABLE 3.6
ERROR MATRIX FOR THE EVALUATION DATA SET OF THE NEURAL NETWORK BASED ON THE
21x21 WINDOW TEXTURAL APPROACH

	Reference Data							
	Dark field	Medium dark field	Light field	Fallow	Pine forest	Hardwood forest	Water	Total
Dark field	22	4	0	0	0	0	0	26
Medium dark field	3	21	3	0	0	0	0	27
Light field	0	0	22	0	0	0	5	27
Fallow	0	0	0	20	0	0	0	20
Pine forest	0	0	0	0	25	0	0	25
Hardwood forest	0	0	0	5	0	25	0	30
Water	0	0	0	0	0	0	20	20
Total	25	25	25	25	25	25	25	175
Producer's Accuracy (%)	88	84	88	80	100	100	80	89[a]
User's Accuracy (%)	85	78	82	100	100	83	100	

[a] – Overall accuracy (%)

TABLE 3.7

COMPARISON OF THE AVERAGE VALUES OF INVERSE DIFFERENCE MOMENT FOR RED, GREED AND BLUE PIXELS FOR VARIOUS CLASSES

	Combination		
Class	Red	Green	Blue
Dark field	0.09	0.10	0.08
Medium dark field	0.06	0.07	0.05
Light field	0.06	0.06	0.05
Fallow	0.04	0.03	0.02
Pine forest	0.03	0.04	0.02
Hardwood forest	0.03	0.03	0.02
Water	0.24	0.12	0.08

TABLE 3.8

COMPARISON OF THE PRODUCER'S ACCURACY (%) FOR ANALYSIS BASED ON VARIOUS COMBINATIONS OF TEXTURAL PARAMETERS

	Combination						
Class	ASM[a], IDM[b], Contr[c], Entr[d], Mean & SD[e]	ASM, IDM, Contr, Entr & SD	ASM, IDM, Contr, Entr & Mean	ASM, IDM, Contr & Entr	ASM, IDM, Contr, Mean & SD	ASM, IDM, Entr, Mean & SD	ASM, IDM, Mean & SD
Dark field	88	80	88	80	64	72	76
Medium dark field	84	80	76	80	76	80	88
Light field	88	88	84	92	88	80	88
Fallow	80	28	80	28	52	36	60
Pine forest	100	100	100	100	100	100	100
Hardwood forest	100	100	100	100	100	92	100
Water	80	80	76	84	72	72	72
Overall accuracy	89	79	86	80	79	76	83

[a] – Angular second moment
[b] – Inverse difference moment
[c] – Contrast
[d] – Entropy
[e] – Standard deviation

TABLE 3.9

COMPARISON OF THE PRODUCER'S ACCURACY (%) FOR ANALYSIS BASED ON VARIOUS COMBINATIONS OF THE HISTOGRAM, TEXTURAL AND SPATIAL APPROACHES

| Class | Combination | | | |
	Histogram & Textural	Textural & Spatial	Histogram & Spatial	Histogram, Textural & Spatial
Dark field	52	48	76	52
Medium dark field	80	76	80	84
Light field	80	92	60	80
Fallow	40	32	84	36
Pine forest	96	100	88	100
Hardwood forest	92	100	84	88
Water	60	68	80	40
Overall accuracy	71	74	79	69
Standard Deviation	21	26	9	25

TABLE 3.10

AVERAGE NETWORK OUTPUT FROM A PNN FOR THE 25 PATTERNS FROM EACH CLASS IN THE EVALUATION DATASET FOR TEXTURAL PARAMETER APPROACH

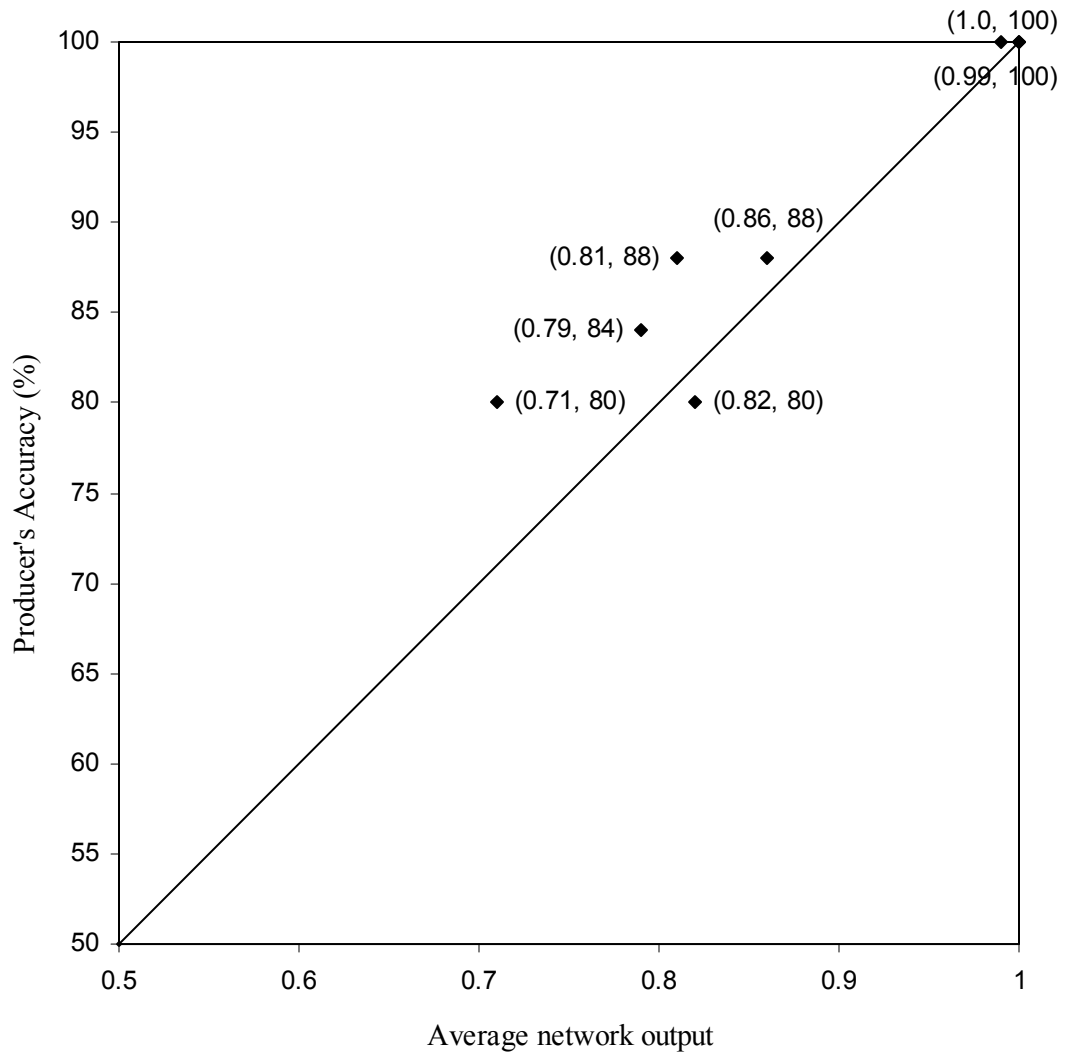| Class	Average network output	Misclassification	Average network output *
Dark field	0.86	Medium dark field	0.14
Medium dark field	0.79	Dark field	0.19
Light field	0.81	Medium dark field	0.18
Fallow	0.71	Hardwood forest	0.29
Pine forest	1.00	-	-
Hardwood forest	0.99	-	-
Water	0.82	Light field	0.18

* average network outputs less than 0.02 were neglected

Fig. 3.1. Average network output for the seven classes on the evaluation data set versus Producer's accuracy for textural approach (coordinates of each point are in paranthesis).

CHAPTER 4

SUMMARY AND FUTURE WORK

In this study, three different approaches to preparing inputs to ANNs for image classification based on ANNs were evaluated on gray-scale and multispectral aerial images. These included histograms of the pixel intensities, textural parameters extracted from the image, and matrices of the pixels for spatial information. All three approaches were tested based on window sizes. Good results were obtained using the ANN based solely on textural parameters. Textural parameters had the highest overall accuracy of the three approaches for the evaluation data set of gray-scale (92%) and multispectral (89%) images, compared to approaches based on histogram and spatial information. The overall accuracy did not improve by using ANNs based on combinations of histogram, spatial and textural information. Textural parameters also had the smallest standard deviation for the producer's accuracy in both gray-scale and multispectral imagery, which further shows consistently good performance by the textural approach. The accuracy for the classification of multispectral images using ANNs for land-use was comparable to previous observations (Yoshida and Omatu, 1994; Paola and Schowengerdt, 1995). The better performance of the textural approach for multispectral images compared to other approaches is consistent with the results of previous studies based using gray-scale and multispectral images (Weszka et al., 1976; Marceau et al., 1990; Singh and Singh, 2001).

The most frequent misclassification in multispectral images was of field areas and water into one another. This can possibly be solved by selectively using histogram approach for them, as the histogram approach showed high accuracy for these classes. Certain classes perform better by using some approach selectively, for example, the textural approach worked the best for forest classes. Edge detection prior to classification can help automate the process of image selection and GUI can facilitate the system's use.

REFERENCES

Baraldi, A., and Parmiggiani, F., 1990. Urban area classification by mulitspectral SPOT images, IEEE Trans. Geosci. Remote Sensing 28 (4), 674-680.

Benediktsson, J. A., Swain, P. H., and Ersoy, O. K., 1990. Neural network approaches versus statistical methods in classification of multisource remote sensing data, IEEE Trans. Geosci. Remote Sensing 28 (4), 540-551.

Bischof, H., Schneider, W., and Pinz, A. J., 1992. Multispectral classification of Landsat-images using neural networks, IEEE Trans. Geosci. Remote Sensing 30 (3), 482-490.

Blackard, J. A., and Dean, D. J., 1999. Comparative accuracies of artificial neural networks and discriminant analysis in predicting forest cover types from cartographic variables, Comput. Electron. Agric. 24, 131-151.

Carmel, Y., and Kadmon, R., 1998. Computerized classification of Mediterranean vegetation using panchromatic aerial photographs, Journal of Vegetation Science 9 (3), 445-454.

Chen, Y. Q., Nixon, M. S., and Thomas, D. W., 1995. Statistical geometrical features for texture classification, Pattern Recognition 28 (4), 537-552.

Civco , D. L. and Waug, Y., 1994. Classification of multispectral, multitemporal, multisource spatial data using artificial neural networks, in Proc. 1994 Annual ASPRS/ACSM Convention, Reno, NV, USA, pp. 123-133.

Cortijo, F. J. and De la Blanca, N. P., 1998. Improving classical contextual classifications, Int. J. Remote Sensing 19 (8), 1591-1613.

Du, L., 1996. Fuzzy classification of earth terrain covers using complex polarimetric SAR data, Int. J. Remote Sensing 17 (4), 809-826.

Fung, T. and Chan, K., 1994. Spatial composition of spectral classes: a structural approach for image analysis of heterogeneous land-use and land-cover types, Photogramm. Eng. Remote Sens. 60 (2), 173-180.

Giraudel, J. L., 2001. A comparison of self-organizing map algorithm and some conventional statistical methods for ecological community ordination, Ecological Modelling 146 (1-3), 329-339.

Gong, P. and Howarth, P. J., 1992. Frequency based contextual classification and gray-level vector reduction for land-use identification, Photogramm. Eng. Remote Sens. 58 (4), 423-437.

Gopal, S. and Woodcock, C., 1994. Theory and methods for accuracy assessment of thematic maps using fuzzy sets, Photogramm. Eng. Remote Sens. 60 (2), 181-188.

Haralick, R. M., Shanmugam, K., and Dinstein, I., 1973. Textural features for image classification, IEEE Trans. Syst., Man, and Cybern. 3 (6), 610-621.

Irons, J. R. Markham, B. L., Nelson, R. F., Toll, D. L., Williams, D. L., Latty, R. S., Stauffer, M. L., 1985. The effect of spatial resolution on the classification of Thematic Mapper data, Int. J. Remote Sensing 6 (8), 1385-1403.

Jensen, J. R., 1979. Spectral and textural features to classify elusive land cover at the urban fringe, Professional Geographer 31 (4), 400-409.

Kondo, N., Ahmad, U., Monta, M., and Murase, H., 2000. Machine vision based quality evaluation of Iyokan orange fruit using neural networks, Comput. Electron. Agric. 29, 135-147.

Lee, J., Weger, R. C., Sengupta, S. K., and Welch, R. M., 1990. A neural network approach to cloud classification, IEEE Trans. Geosci. Remote Sensing 28 (5), 846-855.

Luo, X., Jayas, D. S., and Symons, S. J., 1999. Comparison of statistical and neural network methods for classifying cereal grains using machine vision, Trans. of the ASAE 42 (2), 413-419.

Marceau, D. J., Howarth, P. J., Dubois, J. M., and Gratton, D. J., 1990. Evaluation of the gray-level co-occurrence matrix method for land cover classification using SPOT imagery, IEEE Trans. Geosci. Remote Sensing 28 (4), 513-519.

Mather, P. M., 1990. Theoretical problems in image classification, In: Clark, J. A. and Sevens, M. D. (Eds.), Application of Remote Sensing in Agriculture, London, Butterworths, pp. 127-135.

Metzler, V., Palm, C., Lehmann, T., and Aach, T., 2000. Texture classification of graylevel images by multi cross-coocurrence matrices, in Proc. 15th International Conference on Pattern Recognition, Barcelona, Spain , pp. 549-552.

Moshou, D., Vrindts, E., De Ketelaere, B., De Baerdemaeker, J., and Ramon, H., 2001. A neural network based plant classifier, Comput. Electron. Agric. 31 (1), 5-16.

Paola, J. D. and Schowengerdt, R. A., 1995. A detailed comparison of neural network and maximum likelihood classifiers for urban land use classification, IEEE Trans. Geosci. Remote Sensing 33 (4), 981-996.

Papin, C., 2002. Unsupervised segmentation of low clouds from infrared METEOSAT images based on a contextual spatio-temporal labeling approach, IEEE Trans. Geosci. Remote Sensing 40 (1), 104-114.

Ritter, N. D. and Hepner, G. F., 1990. Application of an artificial neural network to land-cover classification of thematic mapper imagery, Computers and Geosciences 16 (6), 873-880.

Salu, Y. and Tilton, J., 1993. Classification of multispectral image data by the binary diamond neural network and by nonparametric, pixel-by-pixel methods, IEEE Trans. Geosci. Remote Sensing 31 (3), 606-617.

Short, N. M., 1999. Remote sensing tutorial, Available Online:

http://rst.gsfc.nasa.gov/start.html.

Schultz, A., Wieland, R., and Lutze, G., 2000. Neural network in agroecological modeling – stylish application or helpful tool?, Comput. Electron. Agric., 29, 73-97.

Singh, M. and Singh, S., 2001. Evaluation of texture methods for image analysis," Proc. 7th Australian and New Zealand Intelligent Information Systems Conference (18-21 November, 2001), Perth, Australia, pp. 117-121.

Tsai, F., 2002. A derivative-aided hyperspectral image analysis system for land-cover classification. IEEE Trans. Geosci. Remote Sensing 40 (2), 416-425.

Wang, F., 1990. Fuzzy Supervised Classification of Remote Sensing Images, IEEE Trans. Geosci. Remote Sensing 28 (2), 194-201.

Warner, T. A. and Shank, M., 1997. An evaluation of the potential for fuzzy classification of multispectral data using artificial neural networks, Photogramm. Eng. Remote Sens. 63 (11), 1285-1294.

Weszka, J. S., Dyer C. R., and Rosenfeld, A., 1976. A comparative study of texture measures for terrain classification, IEEE Trans. Syst., Man, and Cybern. 6 (4), 269-285.

Yoshida, T. and Omatu, S., 1994. Neural network approach to land cover mapping, IEEE Trans. Geosci. Remote Sensing 32 (5), 1103-1109.

Zhang, J. and Foody, G. M., 2001. Fully-fuzzy supervised classification of sub-urban land cover from remotely sensed imagery: statistical and artificial neural network approaches, Int. J. Remote Sensing 22 (4), 615-628.